THE JOURNAL OF BIOLOGICAL CHEMISTRY VOL. 288, NO. 17, pp. 11761–11770, April 26, 2013
© 2013 by The American Society for Biochemistry and Molecular Biology, Inc. Published in the U.S.A.

Bile Acid Receptor Activation Modulates Hepatic Monocyte Activity and Improves Nonalcoholic Fatty Liver Disease*

Received for publication, December 21, 2012 Published, JBC Papers in Press, March 4, 2013, DOI 10.1074/jbc.M112.446575

Rachel H. McMahan[‡], Xiaoxin X. Wang[§], Lin Ling Cheng[‡], Tibor Krisko[¶], Maxwell Smith[‖], Karim El Kasmi[**], Mark Pruzanski[‡‡], Luciano Adorini[§§], Lucy Golden-Mason[‡¶¶], Moshe Levi[§], and Hugo R. Rosen[‡¶¶1]

From the Divisions of [‡]Gastroenterology and [§]Nephrology and Hypertension, Department of Medicine, and [**]Division of Gastroenterology, Hepatology and Nutrition, Department of Pediatrics, University of Colorado Denver, Aurora, Colorado 80045, the [¶]Division of Gastroenterology, Hepatology and Endoscopy, Brigham and Women's Hospital, Boston, Massachusetts 02115, the [‖]Department of Laboratory Medicine and Pathology, Mayo Clinic Arizona, Scottsdale, Arizona 85259, [‡‡]Intercept Pharmaceuticals, New York, New York 10013, [§§]Intercept Pharmaceuticals, 06073 Perugia, Italy, and the [¶¶]Integrated Program in Immunology, National Jewish Hospital, Denver, Colorado 80206

Background: The bile acid receptors FXR and TGR5 have pleiotropic functions, including immune modulation.
Results: Treatment of a murine model of nonalcoholic fatty liver disease (NAFLD) with a dual FXR/TGR5 agonist decreased intrahepatic inflammation and altered the immune phenotype of monocytes.
Conclusion: Bile acid receptor activation improves NAFLD.
Significance: These results identify potential targeting strategies for treatment of NAFLD.

Nonalcoholic fatty liver disease (NAFLD) affects a large proportion of the American population. The spectrum of disease ranges from bland steatosis without inflammation to nonalcoholic steatohepatitis and cirrhosis. Bile acids are critical regulators of hepatic lipid and glucose metabolism and signal through two major receptor pathways: farnesoid X receptor (FXR), a member of the nuclear hormone receptor superfamily, and TGR5, a G protein-coupled bile acid receptor (GPBAR1). Both FXR and TGR5 demonstrate pleiotropic functions, including immune modulation. To evaluate the effects of these pathways in NAFLD, we treated obese *db*/*db* mice with a dual FXR/TGR5 agonist (INT-767) for 6 weeks. Treatment with the agonist significantly improved the histological features of nonalcoholic steatohepatitis. Furthermore, treatment increased the proportion of intrahepatic monocytes with the anti-inflammatory Ly6C^{low} phenotype and increased intrahepatic expression of genes expressed by alternatively activated macrophages, including CD206, *Retnla*, and *Clec7a*. *In vitro* treatment of monocytes with INT-767 led to decreased Ly6C expression and increased IL-10 production through a cAMP-dependent pathway. Our data indicate that FXR/TGR5 activation coordinates the immune phenotype of monocytes and macrophages, both *in vitro* and *in vivo*, identifying potential targeting strategies for treatment of NAFLD.

Nonalcoholic fatty liver disease (NAFLD)[2] is estimated to affect one-third of the American population (1–3). The spectrum of disease encompasses bland steatosis without inflammation to nonalcoholic steatohepatitis (NASH), the latter being associated with a relatively greater risk of cirrhosis, occurring in up to 15% of patients (4). Although insulin resistance and its sequelae, *i.e.* inappropriate peripheral lipolysis and *de novo* lipogenesis in the liver (5), represent important risk factors for the development of NAFLD, the precise mechanisms controlling the disease pathogenesis remain largely undefined.

Macrophages and monocyte populations are an important source of cytokines in the liver and key players in NASH progression and resolution (6). Indeed, recent data indicate that depletion of Kupffer cells prevents the development of diet-induced steatosis and insulin resistance (7). In addition, the recruitment of different monocyte populations can also affect the balance of M1/M2 macrophages during inflammation. Two subsets of monocytes have been identified, Ly6C^{high} and Ly6C^{low}, which can migrate to tissues and differentiate into pro- or anti-inflammatory macrophages, respectively (8). Obesity and diet-induced increases in the Ly6C^{high} monocyte population have been observed, and adoptive transfer of the Ly6C^{high} monocytes cells causes liver damage (9, 10).

Bile acids are critical regulators in lipid and glucose metabolism and signal through two major receptor pathways: farnesoid X receptor (FXR), a member of the nuclear hormone receptor superfamily (11), and TGR5, a G protein-coupled receptor (12, 13). FXR is considered a master regulator of the pleiotropic activities of endogenous bile acids in enterohepatic recycling and feedback regulation of bile acid synthesis in the gut-liver axis, in gluconeogenesis and glycogenolysis in the liver, and in the regulation of peripheral insulin sensitivity in adipose tissue (11). The relevance of FXR to hepatic physiology has been indicated by the observation that FXR-depleted mice on a high-fat diet exhibit massive hepatic steatosis, necroinflammation, and fibrogenesis (14–16). The demonstration that mice knocked out for both the LDL receptor and FXR and fed a high-fat diet

* This work was supported, in whole or in part, by National Institutes of Health Grant U19 AI 1066328 (to H. R. R.). This work was also supported by Veterans Affairs Merit Review grants (to H. R. R.).
[1] To whom correspondence should be addressed: Div. of Gastroenterology, Dept. of Medicine, University of Colorado Anschutz Medical Campus, B-158, 12631 E. 17th Ave., Aurora, CO 80045. Tel.: 303-724-1858; Fax: 303-724-1891; E-mail: hugo.rosen@ucdenver.edu.
[2] The abbreviations used are: NAFLD, nonalcoholic fatty liver disease; NASH, nonalcoholic steatohepatitis; FXR, farnesoid X receptor; AAM, alternatively activated macrophage(s); MCP-1, monocyte chemoattractant protein-1; sIL-1ra, soluble IL-1 receptor antagonist.

develop necroinflammation and greater hepatic levels of proinflammatory cytokines, TGFβ, procollagen, and collagen compared with LDL receptor$^{-/-}$/FXR$^{+/+}$ mice implicates a role for FXR in determining the features typical of NASH (15). Furthermore, FXR exerts homoeostatic functions at the interface between nutrient and lipid metabolism with innate immunity, antagonizing NF-κB in hepatic inflammatory responses (17) and inhibiting intestinal inflammatory responses (16, 18).

Activation of TGR5 by natural and synthetic bile acids leads to stimulation of cAMP synthesis (19), and phosphorylation of cAMP response element-binding protein results in the transcriptional activation of multiple pathways that include increased GLP-1 (glucagon-like peptide-1) and insulin secretion (20). Stimulation of TGR5 with taurolithocholate attenuates LPS-induced up-regulation of proinflammatory cytokines (IL-1β, IL-6, and TNFα) by rat Kupffer cells (21). Moreover, human THP-1 cells transduced with TGR5 and stimulated with bile acids demonstrate diminished LPS-induced TNFα secretion compared non-transduced cells (13). Agonist-induced TGR5 activation inhibits the expression of inflammatory mediators in response to TLR4 (Toll-like receptor 4) activation by LPS in WT but not TGR5$^{-/-}$ mouse liver, identifying TGR5 as a negative regulator of liver inflammation (22).

In this context, we hypothesized that bile acid receptor activation would ameliorate histology in a murine model of NAFLD/NASH, and we comprehensively explored changes in the phenotype and function of hepatic innate immune cells. By using a combination of pharmacological and genetic approaches, we demonstrate that simultaneous activation of FXR/TGR5 with the dual agonist INT-767 improves NAFLD/NASH histological features, results in recruitment of Ly6C^{low} monocytes to the liver, directly down-regulates the expression of Ly6C on bone marrow-derived monocytes, and decreases production of proinflammatory cytokines by macrophages. Additionally, treatment with INT-767 increases IL-10 production by macrophages and enhances hepatic expression of genes associated with alternatively activated macrophages (AAM). These findings underscore the critical roles played by the bile acid receptor pathways in the pathogenesis of NAFLD/NASH and provide a rationale for them as emerging molecular targets (23) with beneficial effects on lipid metabolism and innate immune responses.

EXPERIMENTAL PROCEDURES

Animals—Male *db*/*db*, *db*/*m*, and C57BL/6 mice were purchased from the Jackson Laboratory. Twelve-week-old *db*/*db* and *db*/*m* mice were fed for 6 weeks with either normal chow only or chow containing the semisynthetic dual FXR/TGR5 agonist 6α-ethyl-24-nor-5β-cholane-3α,7α,23-triol-23-sulfate sodium salt (INT-767, Intercept Pharmaceuticals, New York, NY) at 30 mg/kg of body weight (24). Alternatively, mice were injected intraperitoneally daily with 20 mg/kg INT-767 resuspended in 1% methyl cellulose. All animal experiments were performed humanely under a protocol approved by the Animal Care and Use Committee of the University of Colorado Denver.

Liver Pathology—Serial liver sections were stained with H&E and Masson's trichrome stain using standard techniques. Blinded liver samples were scored by two separate pathologists for NAFLD severity as described previously (25). Briefly, livers were scored for hepatic steatosis as follows: 0, <5% of the liver parenchyma; 1, 5–33% of the liver parenchyma; 2, 33–66% of the liver parenchyma; and 3, >66% of the liver parenchyma. Lobular inflammation was scored by assessment of the number of inflammatory foci within a 20× field: 0, no foci; 1, <2 foci per 20× field; 2, 2–4 foci per 20× field; and 3, >4 foci per 20× field. Livers with no hepatocyte ballooning were give a score of 0, those with a few ballooning cells were given a score of 1, and those with many ballooning cells were given a score of 3.

Isolation of Splenic and Intrahepatic Leukocytes—For isolation of intrahepatic leukocytes, explanted tissue was finely minced and homogenized with a 10-cc syringe, followed by 1-h incubation with digestion medium (0.02% (w/v) collagenase IV and 0.002% DNase) at 37 °C. Red blood cells were lysed in 0.16 M NH_4Cl and 0.17 M Tris (pH 7.65), and the cells were washed twice with RPMI 1640 medium (Invitrogen) containing 10% fetal bovine serum (HyClone). Cells were then filtered through a 70-μm filter and, if not being used immediately, frozen in FBS and 10% Me_2SO. Mouse splenocytes were harvested in a similar manner but without collagenase digestion. Monocytes were isolated from the bone barrow of C57BL/6 mice using the EasySep mouse monocyte enrichment kit (Stem Cell Technologies).

Flow Cytometric Analysis—Directly conjugated antibodies against the following surface molecules were used: CD45 (30-F11), Ly6C (AL21), and Ly6G (1A8) (BD Biosciences). Antibodies against CD115 (AFS98), CD11b (M1/70), CD11c (N418), F4/80 (BM8), and PD-L1 (MIH5) were from eBioscience. The anti-CD206 antibody was from AbD Serotec. Multiparameter flow cytometry was performed using a BD FACSCanto instrument (BD Biosciences) compensated with single fluorochromes and analyzed using FACSDiva software (BD Biosciences). Splenocytes and intrahepatic leukocytes were analyzed for cell surface antigen expression following staining with antibodies at 4 °C in the dark for 30 min. Cells were washed three times with 2 ml of PBS containing 1% bovine serum albumin and 0.01% sodium azide and subsequently fixed in 200 μl of 1% paraformaldehyde (Sigma-Aldrich).

Quantitative PCR—Liver tissue was snap-frozen following harvest and stored in liquid nitrogen until used. Tissues were homogenized (Tissue-Tearor), and RNA was extracted using the RNeasy minikit and converted to cDNA using the QuantiTect RT kit (both from Qiagen) following standard protocols. Real-time quantitative PCR was carried out on an Applied Biosystems 7300 real-time PCR system. The following QuantiTect primer pairs were purchased from Qiagen: procollagen 1A, α-smooth muscle actin, IL-18, TNFα, monocyte chemoattractant protein-1 (MCP-1), IL-1β, CD206, *Retnla*, *Clec7a*, soluble IL-1 receptor antagonist (sIL-1Ra), and F4/80. Samples were run in duplicate in a 10-μl reaction volume consisting of 5 μl of SYBR Green PCR Mix (Qiagen), 1 μl of the primer set, 0.5 μl of cDNA, and 3.5 μl of H_2O. Cycling conditions consisted of 40 cycles at 94 °C for 15 s, 50 °C for 30 s, and 72 °C for 30 s. Each individual sample was normalized to β-actin, and gene expression was compared with the matched normal mouse fed a low-fat diet. TaqMan quantitative PCR was done to determine IL-10 expression using the following primers: IL-10 (Mm00439614_m1) and

β-actin (Mm00607939_s1) (Applied Biosystems). Samples were run in duplicate in a 20-μl reaction volume consisting of 10 μl of TaqMan Gene Expression Master Mix (Applied Biosystems), 1 μl of the primer/probe set, 1 μl of cDNA, and 8 μl of H_2O. Cycling conditions consisted of 40 cycles at 95 °C for 15 s and 60 °C for 1 min. -Fold change in transcripts was calculated using the $\Delta\Delta C_T$ method (26).

In Vitro Stimulation of Macrophages—Bone marrow was isolated from the femurs and tibias of mice by flushing with PBS. Bone marrow cells (5×10^5) were plated in 24-well plates with RPMI 1640 medium and 10% FBS containing 30 ng/ml recombinant M-CSF (eBioscience) and, if indicated, 30 μM INT-767. After 5 days, 100 ng/ml LPS was added to the wells for 24 h, and supernatants were collected and stored at −80 °C. For the production of proinflammatory cytokines, the cells were treated with LPS and 20 ng/ml recombinant IFNγ (eBioscience). RNA was isolated using the RNeasy minikit. For cAMP experiments, macrophage stimulation was done in the presence of the adenylyl cyclase inhibitor MDL-2300A (10 μM, Sigma).

cAMP ELISA—Bone marrow-derived macrophages (1×10^6) were cultured in 24-well plates in RPMI 1640 medium containing 1 mM isobutylmethylxanthine (Sigma) and then incubated for 20 min with 30 μM INT-767. The cells were lysed in 500 μl of 0.1 M HCl, and the lysates were analyzed for cAMP levels according to the cAMP ELISA kit instructions (Cayman Chemical).

Assays for Cytokine Production—For analysis of cytokines in the supernatants of cell cultures, Luminex xMAP and ELISA techniques were utilized. For Luminex, samples were transferred to MultiScreen filter plates (Millipore) and assayed for cytokines using Luminex xMAP technology on a Luminex 100 IS system. Quantities of MCP-1 and IL-1β were determined using a MILLIPLEX MAP magnetic bead kit. Duplicate samples and standards were processed according to the kit protocol, opting for overnight incubation with the beads. Standards were mixed and serially diluted 1:2 in tissue culture medium for the maximum detection range. Results were analyzed using five-parameter logistic curves (fluorescence intensity *versus* pg/ml) generated by Luminex 100 IS software (version 2.3). IL-10 production was determined using the mouse IL-10 Ready-Set-Go! ELISA kit (eBioscience) according to the standard protocol.

Statistical Analysis—Results are expressed as the mean ± S.E. Unpaired Student's *t* tests were used to compare differences between groups, and a *p* value of ≤0.05 was considered significant. Prism 5.0 statistical analysis software (GraphPad Software) was used.

RESULTS

Activation of the Bile Acid Receptor Pathways Improves NAFLD—To determine whether activation of bile acid receptors affects obesity-induced hepatic steatosis and inflammation, we administered the dual FXR/TGR5 bile acid receptor agonist INT-767 for 6 weeks to obese *db*/*db* mice or *db*/*m* lean littermate controls. Administration of INT-767 improved hepatic histology with decreased steatosis and inflammatory foci within the liver (Fig. 1). It has been shown previously that obese *db*/*db* mice fail to develop fibrosis unless fed a diet deficient in methionine and choline (27). Accordingly, in our study, the *db*/*db* mice did not show liver fibrosis as assessed by trichrome staining (data not shown). Nonetheless, treatment with INT-767 significantly decreased expression of the procollagen 1A and α-smooth muscle actin profibrotic genes (Fig. 2, *A* and *B*). Expression of the proinflammatory cytokines IL-18 and TNFα has also been shown to be increased in NAFLD (28–30). Treatment of *db*/*db* mice with INT-767 significantly decreased IL-18 and TNFα expression in the liver (Fig. 2, *C* and *D*), suggesting a reversal of the proinflammatory cytokine profile in response to FXR/TGR5 activation. It should be noted that with the 6-week treatment, there was no significant change in body weight or blood glucose between the obese *db*/*db* and INT-767-treated *db*/*db* mice (data not shown).

FXR/TGR5 Activation Results in Increased Intrahepatic Ly6C^{low} Monocytes—It has recently been demonstrated that mice fed a high-fat diet develop intrahepatic infiltration of Ly6C^{high} monocytes and that these cell are crucial for obesity-associated liver inflammation (10). Conversely, the recruitment of Ly6C^{low} monocytes inhibits the inflammatory response associated with lipid-associated diseases, such as obesity and atherosclerosis, and favors mechanisms of tissue repair (31). Ly6C^{low} monocytes exhibit features of anti-inflammatory macrophages and have been shown to differentiate into tolerogenic dendritic-like cells that use PD-L1, a T cell inhibitory molecule important for liver immunoregulation (32, 33). Therefore, we analyzed the phenotype of intrahepatic monocytes, defined phenotypically as CD45$^+$CD11b$^+$Ly6G$^-$, in mice treated with INT-767. We observed an increase in intrahepatic monocytes in both obese *db*/*db* and INT-767-treated *db*/*db* mice (Fig. 3*A*). The monocyte population was not increased in *db*/*m* mice treated with the agonist, suggesting that INT-767 does not increase the recruitment of monocytes to the liver. However, treatment with the agonist led to a decrease in the intrahepatic Ly6C^{high} monocyte population and an increase in the Ly6C^{low} population (Fig. 3, *B* and *C*). Treatment also resulted in an increased proportion of monocytes with the Ly6C^{low} phenotype both in the liver and, to a lesser extent, in the spleen (Fig. 3*D*). The Ly6C^{low} cells were CD11c$^+$ (Fig. 3*E*), in agreement with a previous report (31). Taken together, these data suggest that the agonist alters the phenotype of monocytes in the liver.

To determine whether the observed hepatic decrease in Ly6C^{high} cells induced by INT-767 treatment was due to a direct or indirect effect on monocyte populations, we treated bone marrow-derived monocytes from C57BL/6 mice fed a normal chow diet with the FXR/TGR5 agonist. Following 48 h of stimulation with INT-767, the levels of Ly6C on monocytes were statistically decreased (Fig. 4, *A* and *B*), suggesting that the observed decrease in intrahepatic Ly6C^{high} cells is due to a direct effect on monocytes.

INT-767 Treatment of Monocytes Attenuates Proinflammatory Cytokines and Increases IL-10 Production by Macrophages—CD11b$^+$Ly6C^{high} and CD11b$^+$Ly6C^{low} monocytes have been shown to differentiate into two different subset of macrophages with distinct functional activity (31). CD11b$^+$Ly6C^{high} monocytes give rise to proinflammatory macrophages, whereas CD11b$^+$Ly6C^{low} monocytes represent precursors for "alternatively activated" macrophages (8, 34). We therefore investi-

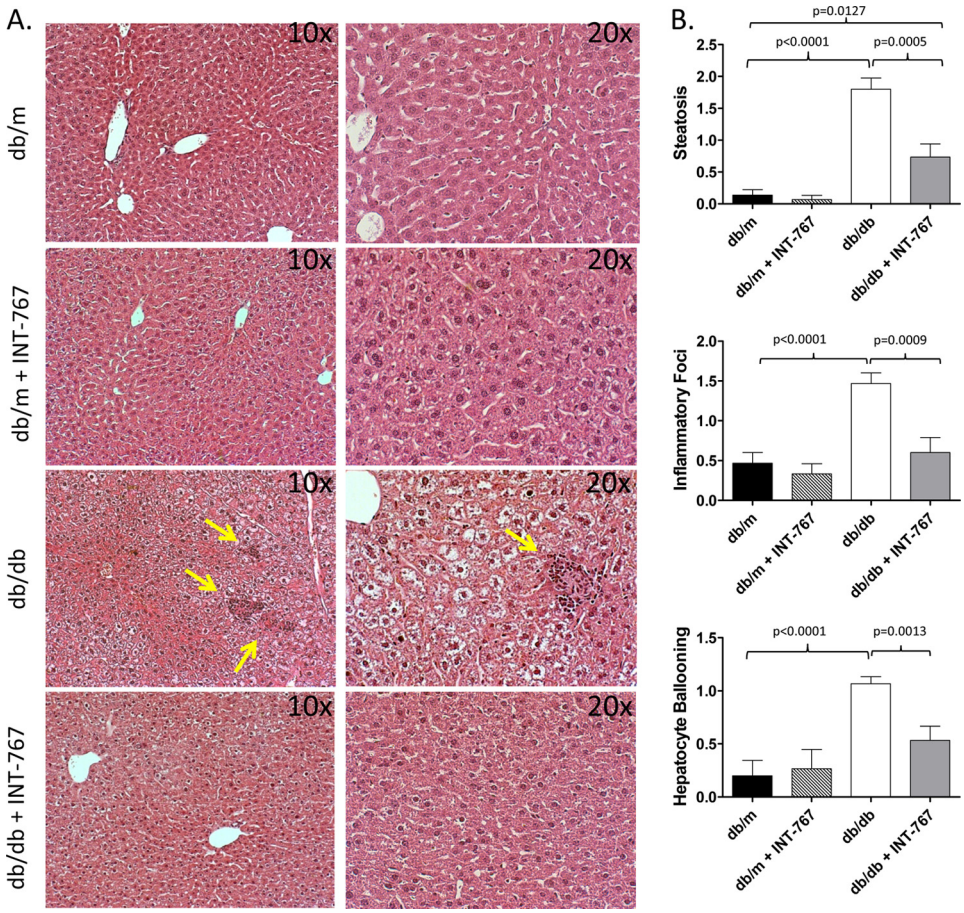

FIGURE 1. **Treatment with the FXR/TGR5 agonist INT-767 improves liver pathology in NAFLD.** Obese *db*/*db* and control *db*/*m* mice were treated with INT-767 (30 mg/kg/day) for 6 weeks. *A*, H&E staining of livers demonstrated increased steatosis and inflammatory foci (*arrows*) in *db*/*db* mice and resolved liver pathology in INT-767-treated mice. *B*, livers from 15 mice/treatment group were scored for steatosis, inflammatory foci, and hepatocyte ballooning as described under "Experimental Procedures." Data are expressed as the arithmetic mean ± S.E.

gated cytokine production from bone marrow-derived macrophages differentiated in the presence of INT-767. Production of the proinflammatory cytokines TNFα and IL-1β and the chemokine MCP-1 was decreased following stimulation with IFNγ and LPS (Fig. 5*A*). Interestingly, INT-767 also increased expression of IL-10 following stimulation with LPS (Fig. 5*B*). A similar increase in IL-10 production following LPS treatment was observed in $CD11b^{+}$ cells isolated from the livers of mice treated intraperitoneally for 8 days with the agonist (Fig. 5*C*).

Treatment with INT-767 Increases Hepatic Expression of Genes Associated with AAM—Because it has been suggested that the $Ly6C^{low}$ monocyte population may differentiate into phagocytes with properties similar to AAM (8), we analyzed the macrophage phenotype in the livers of *db*/*db* mice treated with INT-767 (Fig. 6). Compared with *db*/*m* mice, *db*/*db* mice had higher expression of the F4/80 gene, consistent with an increase in hepatic macrophage population. The expression levels of F4/80 were further increased following treatment with INT-767 (Fig. 6*A*). Macrophages can be characterized as M1 or M2 based on the expression of specific genes (35). Increased levels of genes associated with M2 or AAM, CD206, *Retnla*, and *Clec7a* (dectin-1), were observed in mice treated with INT-767 (Fig. 6*B*). In addition, CD206 was expressed at a higher percentage of intrahepatic macrophages in mice treated with INT-767 (Fig. 6*C*). Expression of sIL-1Ra was also increased in the livers of INT-767-treated mice. Collectively, these data indicate a phenotypic switch from a proinflammatory macrophage to an AAM within the livers of mice treated with the dual FXR/TGR5 agonist INT-767. Importantly, cell surface expression of CD206 and the T cell inhibitory ligand PD-L1 was increased following *in vitro* incubation of bone marrow-derived macrophages with INT-767 (Fig. 6*D*), demonstrating that the agonist can act directly on these cells to alter the phenotype.

INT-767-increased IL-10 Is Mediated through cAMP—Prior work has indicated that cAMP is important for signaling through TGR5, which is a G protein-coupled receptor (36, 37). Therefore, we investigated the role of cAMP signaling in this model. We verified that the INT-767 agonist induced cAMP production from monocytes (Fig. 7*A*). Furthermore, activation of monocyte-derived macrophages with LPS and INT-767 in the presence of MDL-2300A, an adenylyl cyclase inhibitor that inhibits generation of cAMP, attenuated the INT-767-induced increase in IL-10 (Fig. 7*B*).

DISCUSSION

We have shown that treatment of a murine model of NAFLD with a dual FXR/TGR5 bile acid receptor agonist improves disease and alters the phenotype of intrahepatic macrophage populations. Cells of the monocyte/macrophage lineage are highly

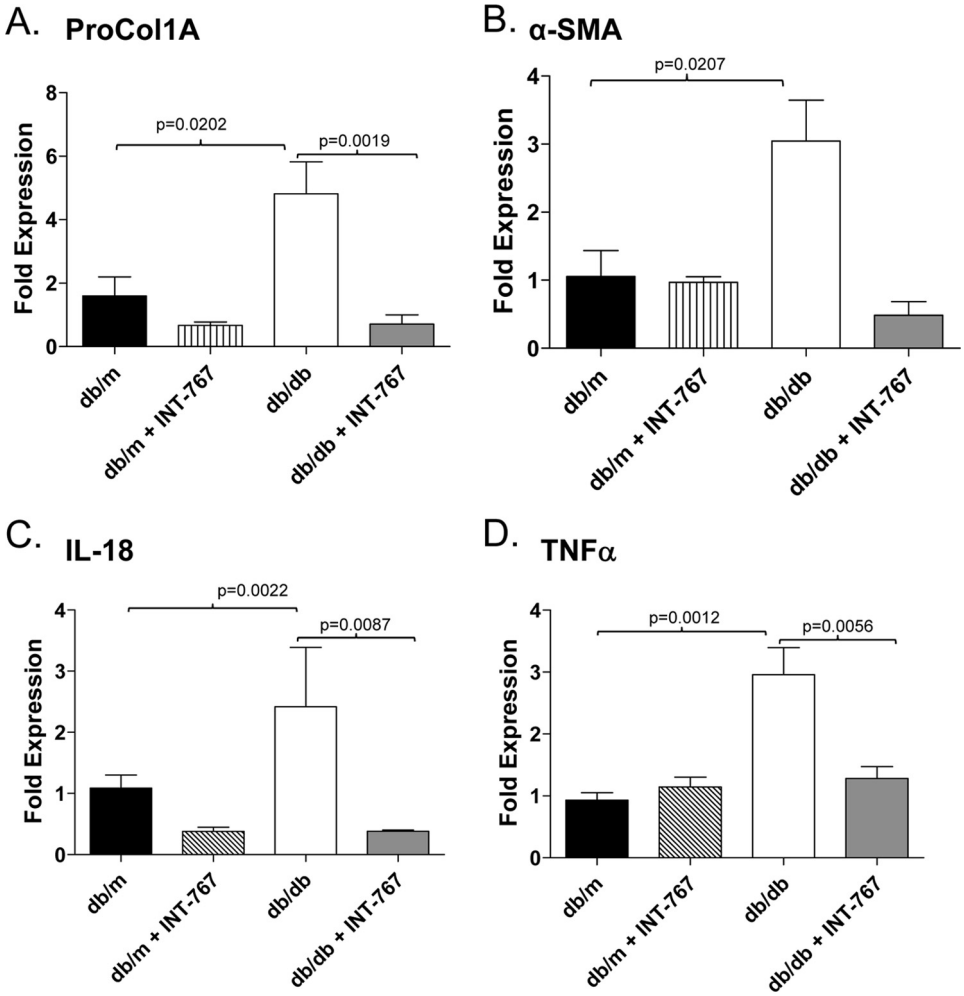

FIGURE 2. **Decreased intrahepatic expression of profibrotic and proinflammatory genes in obese *db*/*db* mice treated with INT-767.** Intrahepatic expression of the indicated profibrotic (*A* and *B*) and proinflammatory (*C* and *D*) genes from *db*/*m* and obese *db*/*db* mice fed INT-767 for 6 weeks was determined by quantitative PCR. Data are expressed as the arithmetic mean ± S.E. of eight mice/treatment group. *p* values represent unpaired *t* tests. *ProCol1A*, procollagen 1A; *α-SMA*, α-smooth muscle actin.

heterogeneous and display remarkable plasticity with regard to cytokine production and immunoregulatory effects (38). A common designation for macrophages divides them into two broad groups, M1 and M2. M1 (or "classically activated") macrophages produce Th1-type cytokines and are induced by IFNγ and Toll-like receptor stimulation. M2 (AAM) macrophages are induced by a variety of stimuli, including the Th2 cytokines IL-4 and IL-13 (35). IL-10 may also be important in the differentiation of M2 macrophages because IL-10 knockout mice have fewer M2 macrophages (39). The M2 subset of macrophages demonstrates extensive functional diversity, including increased phagocytic activity and mannose receptor expression, enhanced IL-10 production, and high expression of the IL-1 decoy receptor (35). In general, these immunoregulatory cells dampen inflammation and promote tissue remodeling, playing an important role during the resolution phase of inflammation by producing anti-inflammatory cytokines (*e.g.* IL-10, TGFβ, and sIL-1Ra) and scavenging cellular debris (40).

We have shown that FXR/TGR5 activation by INT-767 inhibits the production of proinflammatory cytokines from macrophages and decreases intrahepatic expression of both TNFα and IL-18. In other disease models, both FXR and TGR5 activation has been shown to directly inhibit LPS-induced proinflammatory cytokine and chemokine production by macrophages, including TNFα, IL-1β, IL-6, and MCP-1 (18, 21, 41); this decrease is likely to improve NAFLD given the importance of proinflammatory cytokines in disease pathogenesis (42). In addition to inhibition of proinflammatory cytokine production, we have demonstrated that INT-767, in combination with LPS activation of TLR4 enhances IL-10 production and CD206 expression on macrophages. Treatment also restores expression of M2 markers in the livers of *db*/*db* mice and increases production of IL-10 by intrahepatic macrophages.

Recent data suggest that M2 macrophages may be protective in NAFLD/NASH pathogenesis, as shown by the observation that blocking M2 activation exacerbates obesity-induced insulin resistance and induces NAFLD (43). Co-culture experiments with hepatocytes have previously indicated that impairment of M2 activation leads to potent suppression of β-oxidation and oxidative phosphorylation (43). Although the role of IL-10 in obesity-induced inflammation and liver disease is not fully elucidated, macrophages in the adipose tissue of

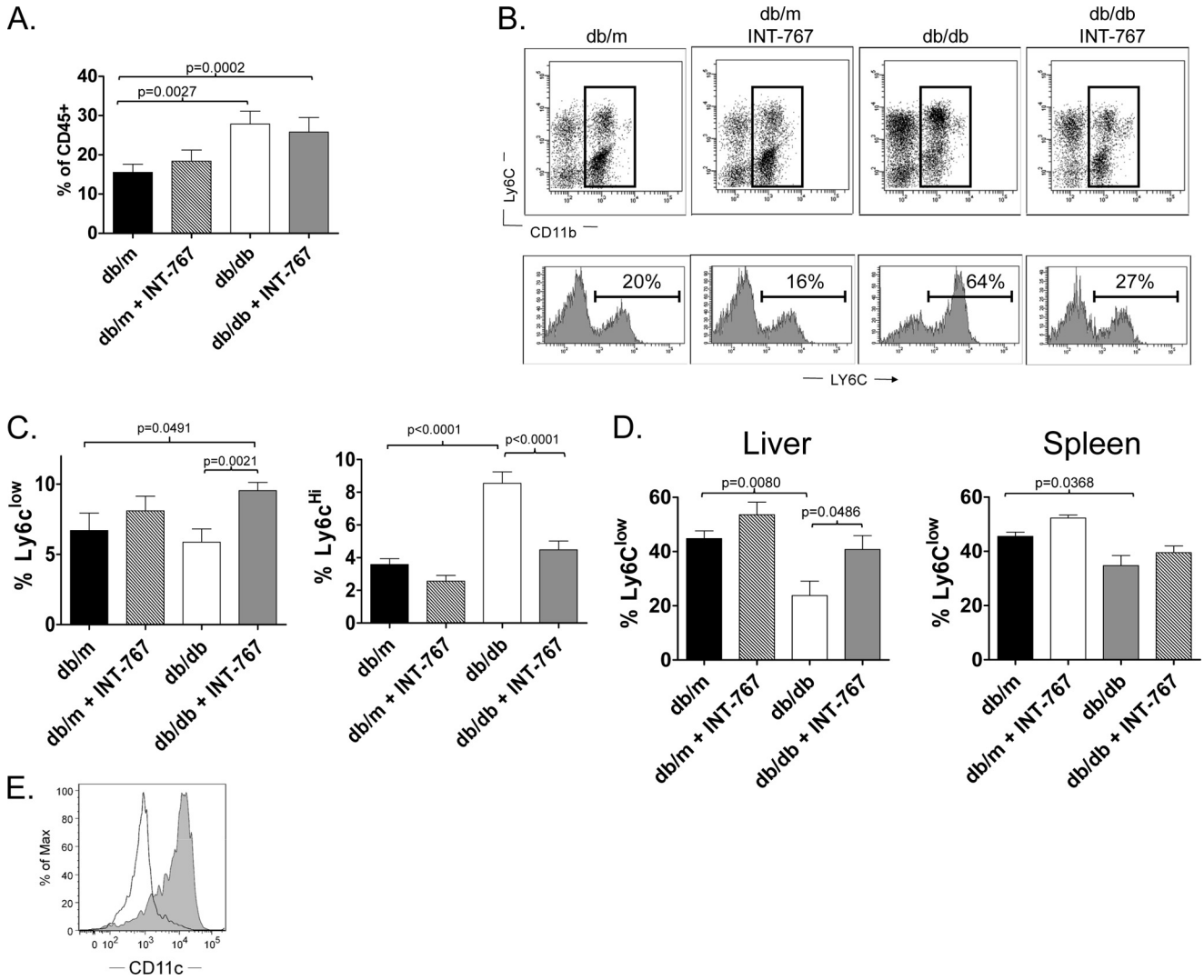

FIGURE 3. **Increased intrahepatic Ly6C^{low} monocytes in obese *db*/*db* mice treated with INT-767.** Intrahepatic monocyte populations from obese *db*/*db* mice treated with INT-767 for 6 weeks were analyzed by flow cytometry. *A*, the percentage of CD45$^+$ cells in the liver that were monocytes (CD115$^+$CD11b$^+$Ly6G$^-$) was increased in mice treated with INT-767. Data represent the mean ± S.E. from 16 mice/treatment group. *B*, *upper*, representative plots show Ly6C and CD11b expression on intrahepatic CD45$^+$F4/80$^-$Ly6G$^-$ cells from *db*/*m* and *db*/*db* mice treated with INT-767. *Lower*, histograms of Ly6C staining are shown for the gated populations. *C*, bar graphs demonstrate the percentage of total CD45$^+$ intrahepatic cells that are Ly6C^{low} (*left*) or Ly6C^{high} (*right*) monocytes. Data represent the mean ± S.E. from 16 mice/treatment group. *D*, bar graphs demonstrate the percentage of monocytes with low expression of Ly6C in the liver (*left*) and spleen (*right*). Treatment with INT-767 significantly increased the number of Ly6C^{low} cells in the livers of *db*/*db* mice. Data represent the mean ± S.E. from 16 mice/treatment group. *E*, a representative histogram plot shows increased CD11c expression on Ly6C^{low} (*gray*) compared with Ly6C^{high} (*black line*) monocytes.

mice fed a high-fat diet undergo a phenotypic switch from IL-10-producing M2 macrophages to TNFα-producing M1 macrophages (44), and the latter are directly linked with insulin resistance (45). Furthermore, mice lacking IL-10 demonstrate more severe liver inflammation and steatosis following a high-fat diet (46, 47), suggesting that IL-10 may play a protective role in NAFLD.

The recruitment of different monocyte populations can also affect the balance of M1/M2 macrophages during inflammation. Two subsets of monocytes, Ly6C^{high} and Ly6C^{low}, have been identified that can migrate to tissues and differentiate into pro- or anti-inflammatory macrophages, respectively (8). Obesity and diet-induced increases in the Ly6C^{high} monocyte population have been observed, and adoptive transfer of the Ly6C^{high} monocyte cells causes liver damage (9, 10). In keeping with these observations, we found an increase in the Ly6C^{high} monocyte population in *db*/*db* mice. This increase was reversed following treatment with INT-767, and *in vitro* treatment of monocytes directly down-regulated Ly6C expression. Therefore, treatment with INT-767 may also modulate the phenotype of monocytes recruited to the steatotic liver by inducing a switch from Ly6C^{high} to Ly6C^{low} monocytes and therefore altering the macrophage populations in the liver.

The signaling pathways downstream of FXR and TGR5 that modulate macrophage function have not been fully elucidated, but FXR has been shown to antagonize NF-κB, which may explain its inhibitory actions against proinflammatory cytokines (17). Additionally, TGR5 has been shown to induce cAMP production by macrophages (13), and this pathway is important for IL-10 production (48). Here, we have shown that the INT-767 agonist increases cAMP production by macrophages and that inhibition of this pathway prevents agonist-induced IL-10

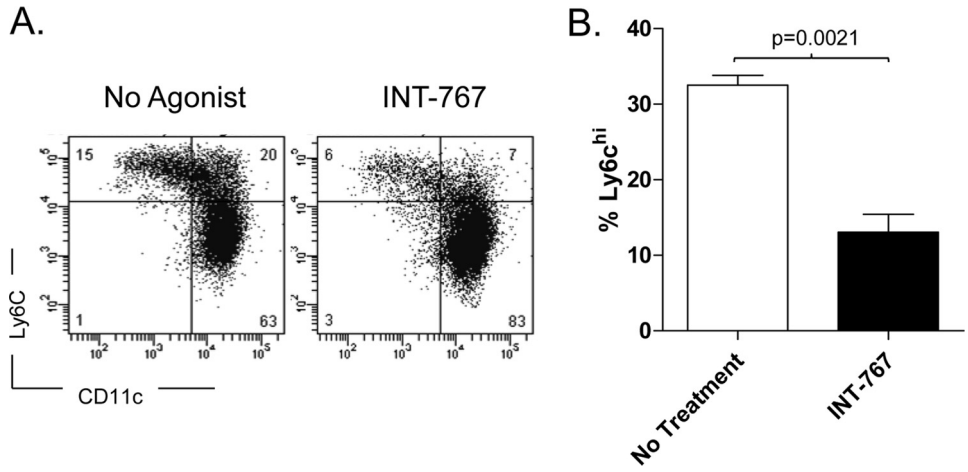

FIGURE 4. **Decreased Ly6C expression by CD115$^+$CD11b$^+$ cells treated *in vitro* with INT-767.** Bone marrow-derived monocytes from C57BL/6J mice were isolated by magnetic bead separation; treated *in vitro* for 48 h with the INT-767 agonist; and stained with antibodies against CD115, CD11b, Ly6G, Ly6C, and CD11c. *A*, representative flow cytometric plots showing down-regulation of Ly-6C on monocytes (CD115$^+$CD11b$^+$Ly6G$^-$). *B*, bar graphs demonstrating the percentage of CD115$^+$CD11b$^+$Ly6G$^-$ cells from bone marrow with high expression of Ly6C. Data represent the mean ± S.E. from triplicate samples.

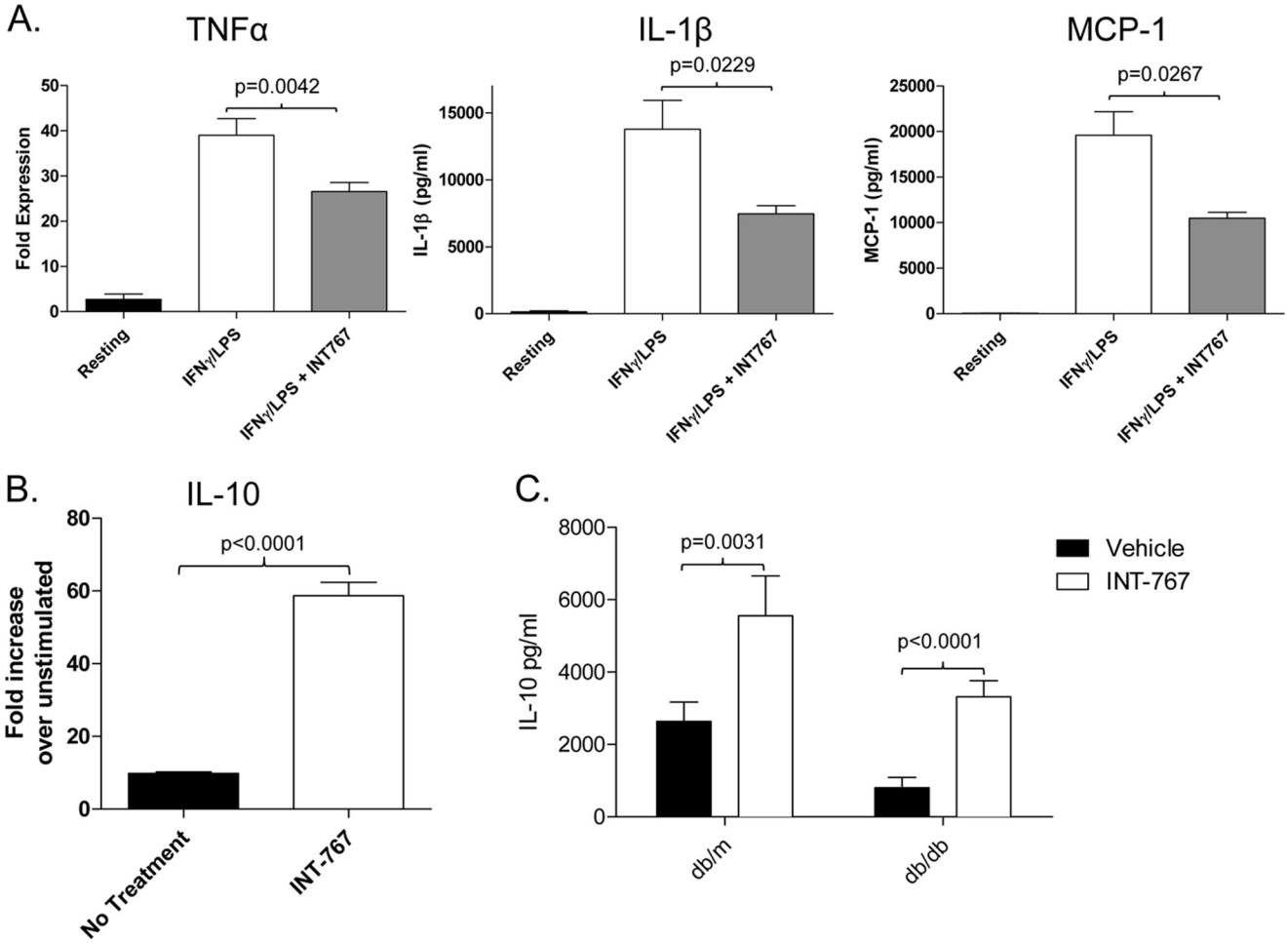

FIGURE 5. **Decreased proinflammatory cytokines and enhanced IL-10 production by macrophages treated *in vitro* with INT-767.** *A*, bone marrow-derived macrophages from C57BL/6 mice were stimulated with 20 ng/ml IFNγ and 100 ng/ml LPS for 24 h, and the relative expression levels of TNFα, MCP-1, and IL-1β were determined by quantitative PCR. Expression was normalized to β-actin expression, and the -fold expression over resting macrophages is shown. *B*, shown is IL-10 gene expression in macrophages matured in the presence of the INT-767 agonist following LPS stimulation. The bar graph represents the mean ± S.E. from two separate experiments. *C*, monocytes were isolated from the livers of *db*/*db* and *db*/*m* mice treated with INT-767 *in vivo* and cultured with 100 ng/ml LPS for 24 h. The presence of IL-10 in the supernatants was determined by ELISA. Data represent triplicate samples from two mice/treatment group.

production (Fig. 7). The observed inhibition of proinflammatory cytokines by TGR5 seen by other groups may be due to IL-10-induced inhibition of proinflammatory cytokine production from macrophages in an autocrine fashion (49). Further studies differentiating the downstream signaling pathways of FXR and TGR5 in macrophages are warranted.

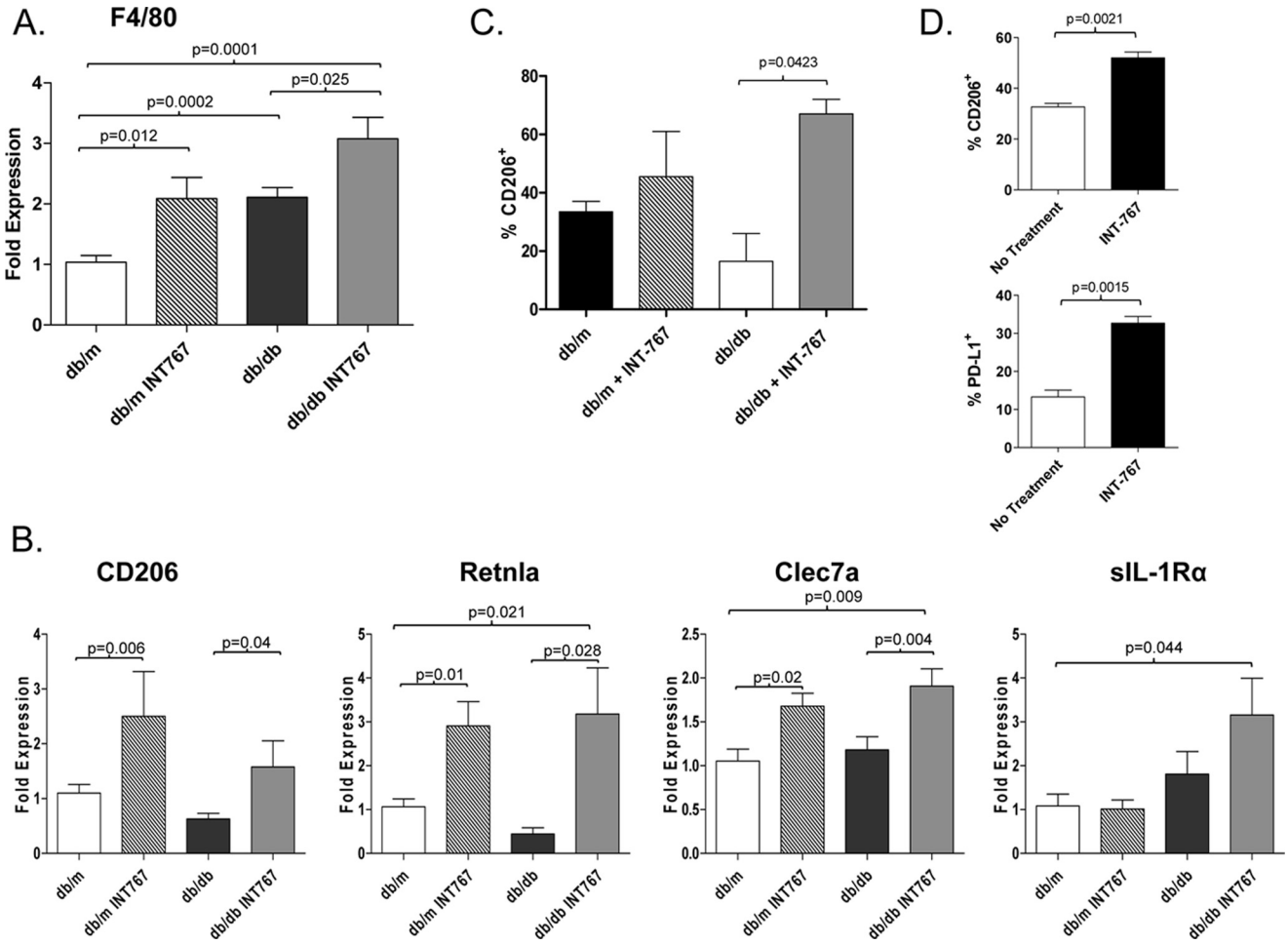

FIGURE 6. **Increased expression of AAM markers by monocytes following INT-767 treatment.** The liver gene expression levels of the macrophage marker F4/80 (*A*) and the markers of alternative activation (CD206, *Retnla*, *Clec7a* and sIL-1Ra) (*B*) were determined in mice treated with the INT-767 agonist for 6 weeks. Expression was normalized against β-actin, and the -fold expression over livers from *db/m* mice was calculated. Data represent the mean ± S.E. from six mice/treatment group with the exception of sIL-1Ra, which was four mice/group. *C*, the percentage of intrahepatic macrophages ($CD45^+CD11b^+F4/80^+Ly6G^-$) expressing CD206 was determined by flow cytometry. Data represent samples from four mice/treatment group. *D*, bone marrow-derived macrophages from C57BL/6 mice were differentiated in the presence of INT-767 and stimulated with 100 ng/ml LPS for 24 h. The percentage of $CD115^+CD11b^+F4/80^+$ cells expressing CD206 and PD-L1 was determined by flow cytometry. The bar graphs present the mean ± S.E. from two separate experiments.

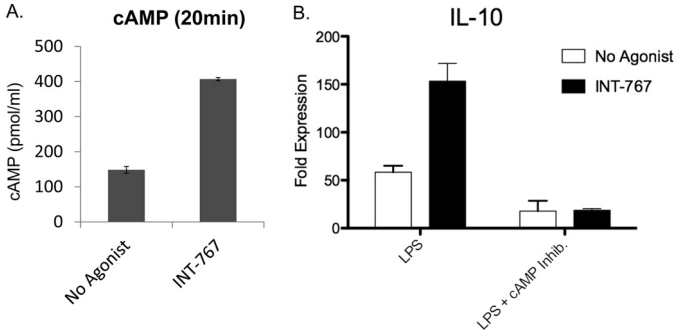

FIGURE 7. **INT-767 induces cAMP production by macrophages, and blocking cAMP inhibits cytokine production.** *A*, bone marrow-derived macrophages from C57BL/6 mice were stimulated with 30 μM INT-767 for 20 min, and cAMP production was determined by ELISA. *B*, macrophages were matured in the presence of the INT-767 agonist, followed by LPS stimulation for 18 h either alone or in the presence of the cAMP inhibitor MDL-2330A. IL-10 expression was determined by quantitative PCR. The bar graphs represent the mean ± S.E.

In conclusion, our data indicate that treatment with a dual FXR/TGR5 agonist decreases liver steatosis and inhibits hepatic inflammation in a murine model of NAFLD. The dual agonist decreases proinflammatory cytokines, increases IL-10 production, leads to down-regulation of Ly6C both *in vitro* and *in vivo*, and results in a phenotypic reversal from obesity-induced M1 to M2 macrophages.

REFERENCES

1. Puri, P., Wiest, M. M., Cheung, O., Mirshahi, F., Sargeant, C., Min, H. K., Contos, M. J., Sterling, R. K., Fuchs, M., Zhou, H., Watkins, S. M., and Sanyal, A. J. (2009) The plasma lipidomic signature of nonalcoholic steatohepatitis. *Hepatology* **50,** 1827–1838
2. Sheth, S. G., Gordon, F. D., and Chopra, S. (1997) Nonalcoholic steatohepatitis. *Ann. Intern. Med.* **126,** 137–145
3. Angulo, P. (2002) Nonalcoholic fatty liver disease. *N. Engl. J. Med.* **346,** 1221–1231
4. Harrison, S. A., Oliver, D., Arnold, H. L., Gogia, S., and Neuschwander-Tetri, B. A. (2008) Development and validation of a simple NAFLD clinical scoring system for identifying patients without advanced disease. *Gut* **57,** 1441–1447
5. Neuschwander-Tetri, B. A. (2010) Hepatic lipotoxicity and the pathogenesis of nonalcoholic steatohepatitis: the central role of nontriglyceride fatty acid metabolites. *Hepatology* **52,** 774–788
6. Baffy, G. (2009) Kupffer cells in non-alcoholic fatty liver disease: the emerging view. *J Hepatol.* **51,** 212–223
7. Huang, W., Metlakunta, A., Dedousis, N., Zhang, P., Sipula, I., Dube, J. J.,

Scott, D. K., and O'Doherty, R. M. (2010) Depletion of liver Kupffer cells prevents the development of diet-induced hepatic steatosis and insulin resistance. *Diabetes* **59,** 347–357
8. Nahrendorf, M., Swirski, F. K., Aikawa, E., Stangenberg, L., Wurdinger, T., Figueiredo, J. L., Libby, P., Weissleder, R., and Pittet, M. J. (2007) The healing myocardium sequentially mobilizes two monocyte subsets with divergent and complementary functions. *J. Exp. Med.* **204,** 3037–3047
9. Swirski, F. K., Libby, P., Aikawa, E., Alcaide, P., Luscinskas, F. W., Weissleder, R., and Pittet, M. J. (2007) Ly-6C^{hi} monocytes dominate hypercholesterolemia-associated monocytosis and give rise to macrophages in atheromata. *J. Clin. Invest.* **117,** 195–205
10. Deng, Z. B., Liu, Y., Liu, C., Xiang, X., Wang, J., Cheng, Z., Shah, S. V., Zhang, S., Zhang, L., Zhuang, X., Michalek, S., Grizzle, W. E., and Zhang, H. G. (2009) Immature myeloid cells induced by a high-fat diet contribute to liver inflammation. *Hepatology* **50,** 1412–1420
11. Lefebvre, P., Cariou, B., Lien, F., Kuipers, F., and Staels, B. (2009) Role of bile acids and bile acid receptors in metabolic regulation. *Physiol. Rev.* **89,** 147–191
12. Maruyama, T., Miyamoto, Y., Nakamura, T., Tamai, Y., Okada, H., Sugiyama, E., Nakamura, T., Itadani, H., and Tanaka, K. (2002) Identification of membrane-type receptor for bile acids (M-BAR). *Biochem. Biophys. Res. Commun.* **298,** 714–719
13. Kawamata, Y., Fujii, R., Hosoya, M., Harada, M., Yoshida, H., Miwa, M., Fukusumi, S., Habata, Y., Itoh, T., Shintani, Y., Hinuma, S., Fujisawa, Y., and Fujino, M. (2003) A G protein-coupled receptor responsive to bile acids. *J. Biol. Chem.* **278,** 9435–9440
14. Musso, G., Gambino, R., and Cassader, M. (2010) Emerging molecular targets for the treatment of nonalcoholic fatty liver disease. *Annu. Rev. Med.* **61,** 375–392
15. Kong, B., Luyendyk, J. P., Tawfik, O., and Guo, G. L. (2009) Farnesoid X receptor deficiency induces nonalcoholic steatohepatitis in low-density lipoprotein receptor-knockout mice fed a high-fat diet. *J. Pharmacol. Exp. Ther.* **328,** 116–122
16. Vavassori, P., Mencarelli, A., Renga, B., Distrutti, E., and Fiorucci, S. (2009) The bile acid receptor FXR is a modulator of intestinal innate immunity. *J. Immunol.* **183,** 6251–6261
17. Wang, Y. D., Chen, W. D., Wang, M., Yu, D., Forman, B. M., and Huang, W. (2008) Farnesoid X receptor antagonizes nuclear factor κB in hepatic inflammatory response. *Hepatology* **48,** 1632–1643
18. Gadaleta, R. M., van Erpecum, K. J., Oldenburg, B., Willemsen, E. C., Renooij, W., Murzilli, S., Klomp, L. W., Siersema, P. D., Schipper, M. E., Danese, S., Penna, G., Laverny, G., Adorini, L., Moschetta, A., and van Mil, S. W. (2011) Farnesoid X receptor activation inhibits inflammation and preserves the intestinal barrier in inflammatory bowel disease. *Gut* **60,** 463–472
19. Fiorucci, S., Mencarelli, A., Palladino, G., and Cipriani, S. (2009) Bile-acid-activated receptors: targeting TGR5 and farnesoid-X-receptor in lipid and glucose disorders. *Trends Pharmacol. Sci.* **30,** 570–580
20. Thomas, C., Gioiello, A., Noriega, L., Strehle, A., Oury, J., Rizzo, G., Macchiarulo, A., Yamamoto, H., Mataki, C., Pruzanski, M., Pellicciari, R., Auwerx, J., and Schoonjans, K. (2009) TGR5-mediated bile acid sensing controls glucose homeostasis. *Cell Metab.* **10,** 167–177
21. Keitel, V., Donner, M., Winandy, S., Kubitz, R., and Häussinger, D. (2008) Expression and function of the bile acid receptor TGR5 in Kupffer cells. *Biochem. Biophys. Res. Commun.* **372,** 78–84
22. Wang, Y. D., Chen, W. D., Yu, D., Forman, B. M., and Huang, W. (2011) The G-protein-coupled bile acid receptor, Gpbar1 (TGR5), negatively regulates hepatic inflammatory response through antagonizing nuclear factor κ light-chain enhancer of activated B cells (NF-κB) in mice. *Hepatology* **54,** 1421–1432
23. Thomas, C., Pellicciari, R., Pruzanski, M., Auwerx, J., and Schoonjans, K. (2008) Targeting bile-acid signalling for metabolic diseases. *Nat. Rev. Drug Discov.* **7,** 678–693
24. Rizzo, G., Passeri, D., De Franco, F., Ciaccioli, G., Donadio, L., Rizzo, G., Orlandi, S., Sadeghpour, B., Wang, X. X., Jiang, T., Levi, M., Pruzanski, M., and Adorini, L. (2010) Functional characterization of the semisynthetic bile acid derivative INT-767, a dual farnesoid X receptor and TGR5 agonist. *Mol. Pharmacol.* **78,** 617–630
25. Kleiner, D. E., Brunt, E. M., Van Natta, M., Behling, C., Contos, M. J., Cummings, O. W., Ferrell, L. D., Liu, Y. C., Torbenson, M. S., Unalp-Arida, A., Yeh, M., McCullough, A. J., and Sanyal, A. J. (2005) Design and validation of a histological scoring system for nonalcoholic fatty liver disease. *Hepatology* **41,** 1313–1321
26. Livak, K. J., and Schmittgen, T. D. (2001) Analysis of relative gene expression data using real-time quantitative PCR and the $2^{-\Delta\Delta CT}$ method. *Methods* **25,** 402–408
27. Sahai, A., Malladi, P., Pan, X., Paul, R., Melin-Aldana, H., Green, R. M., and Whitington, P. F. (2004) Obese and diabetic *db*/*db* mice develop marked liver fibrosis in a model of nonalcoholic steatohepatitis: role of short-form leptin receptors and osteopontin. *Am. J. Physiol. Gastrointest. Liver Physiol.* **287,** G1035–G1043
28. Guebre-Xabier, M., Yang, S., Lin, H. Z., Schwenk, R., Krzych, U., and Diehl, A. M. (2000) Altered hepatic lymphocyte subpopulations in obesity-related murine fatty livers: potential mechanism for sensitization to liver damage. *Hepatology* **31,** 633–640
29. Lin, H. Z., Yang, S. Q., Chuckaree, C., Kuhajda, F., Ronnet, G., and Diehl, A. M. (2000) Metformin reverses fatty liver disease in obese, leptin-deficient mice. *Nat. Med.* **6,** 998–1003
30. Li, Z., Yang, S., Lin, H., Huang, J., Watkins, P. A., Moser, A. B., Desimone, C., Song, X. Y., and Diehl, A. M. (2003) Probiotics and antibodies to TNF inhibit inflammatory activity and improve nonalcoholic fatty liver disease. *Hepatology* **37,** 343–350
31. Domínguez, P. M., and Ardavín, C. (2010) Differentiation and function of mouse monocyte-derived dendritic cells in steady state and inflammation. *Immunol. Rev.* **234,** 90–104
32. Peng, Y., Latchman, Y., and Elkon, K. B. (2009) Ly6C^{low} monocytes differentiate into dendritic cells and cross-tolerize T cells through PDL-1. *J. Immunol.* **182,** 2777–2785
33. Ilkovitch, D., and Lopez, D. M. (2009) The liver is a site for tumor-induced myeloid-derived suppressor cell accumulation and immunosuppression. *Cancer Res.* **69,** 5514–5521
34. Geissmann, F., Jung, S., and Littman, D. R. (2003) Blood monocytes consist of two principal subsets with distinct migratory properties. *Immunity* **19,** 71–82
35. Biswas, S. K., and Mantovani, A. (2010) Macrophage plasticity and interaction with lymphocyte subsets: cancer as a paradigm. *Nat. Immunol.* **11,** 889–896
36. Keitel, V., Cupisti, K., Ullmer, C., Knoefel, W. T., Kubitz, R., and Häussinger, D. (2009) The membrane-bound bile acid receptor TGR5 is localized in the epithelium of human gallbladders. *Hepatology* **50,** 861–870
37. Pols, T. W., Nomura, M., Harach, T., Lo Sasso, G., Oosterveer, M. H., Thomas, C., Rizzo, G., Gioiello, A., Adorini, L., Pellicciari, R., Auwerx, J., and Schoonjans, K. (2011) TGR5 activation inhibits atherosclerosis by reducing macrophage inflammation and lipid loading. *Cell Metab.* **14,** 747–757
38. Gordon, S. (2003) Alternative activation of macrophages. *Nat. Rev. Immunol.* **3,** 23–35
39. Bosschaerts, T., Guilliams, M., Noel, W., Hérin, M., Burk, R. F., Hill, K. E., Brys, L., Raes, G., Ghassabeh, G. H., De Baetselier, P., and Beschin, A. (2008) Alternatively activated myeloid cells limit pathogenicity associated with African trypanosomiasis through the IL-10 inducible gene selenoprotein P. *J. Immunol.* **180,** 6168–6175
40. Gordon, S., and Martinez, F. O. (2010) Alternative activation of macrophages: mechanism and functions. *Immunity* **32,** 593–604
41. Wang, X. X., Jiang, T., Shen, Y., Caldas, Y., Miyazaki-Anzai, S., Santamaria, H., Urbanek, C., Solis, N., Scherzer, P., Lewis, L., Gonzalez, F. J., Adorini, L., Pruzanski, M., Kopp, J. B., Verlander, J. W., and Levi, M. (2010) Diabetic nephropathy is accelerated by farnesoid X receptor deficiency and inhibited by farnesoid X receptor activation in a type 1 diabetes model. *Diabetes* **59,** 2916–2927
42. Maher, J. J., Leon, P., and Ryan, J. C. (2008) Beyond insulin resistance: innate immunity in nonalcoholic steatohepatitis. *Hepatology* **48,** 670–678
43. Odegaard, J. I., Ricardo-Gonzalez, R. R., Red Eagle, A., Vats, D., Morel, C. R., Goforth, M. H., Subramanian, V., Mukundan, L., Ferrante, A. W., and Chawla, A. (2008) Alternative M2 activation of Kupffer cells by

PPARδ ameliorates obesity-induced insulin resistance. *Cell Metab.* **7,** 496–507
44. Lumeng, C. N., Bodzin, J. L., and Saltiel, A. R. (2007) Obesity induces a phenotypic switch in adipose tissue macrophage polarization. *J. Clin. Invest.* **117,** 175–184
45. Odegaard, J. I., and Chawla, A. (2011) Alternative macrophage activation and metabolism. *Annu. Rev. Pathol.* **6,** 275–297
46. Clementi, A. H., Gaudy, A. M., van Rooijen, N., Pierce, R. H., and Mooney, R. A. (2009) Loss of Kupffer cells in diet-induced obesity is associated with increased hepatic steatosis, STAT3 signaling, and further decreases in insulin signaling. *Biochim. Biophys. Acta* **1792,** 1062–1072
47. Cintra, D. E., Pauli, J. R., Araújo, E. P., Moraes, J. C., de Souza, C. T., Milanski, M., Morari, J., Gambero, A., Saad, M. J., and Velloso, L. A. (2008) Interleukin-10 is a protective factor against diet-induced insulin resistance in liver. *J. Hepatol.* **48,** 628–637
48. Foey, A. D., and Brennan, F. M. (2004) Conventional protein kinase C and atypical protein kinase Cζ differentially regulate macrophage production of tumour necrosis factor-α and interleukin-10. *Immunology* **112,** 44–53
49. Huang, H., Park, P. H., McMullen, M. R., and Nagy, L. E. (2008) Mechanisms for the anti-inflammatory effects of adiponectin in macrophages. *J. Gastroenterol. Hepatol.* **23,** S50–S53